Optics Communications 335 (2015) 37–41

Contents lists available at ScienceDirect

Optics Communications

journal homepage: www.elsevier.com/locate/optcom

Nonlinear optical absorption in parabolic quantum well via two-photon absorption process

Huynh Vinh Phuc [a,c,*], Nguyen Ngoc Hieu [a], Le Dinh [b], Tran Cong Phong [b]

[a] Institute of Research and Development, Duy Tan University, Da Nang, Viet Nam
[b] Center for Theoretical and Computational Physics, Hue University, Hue, Viet Nam
[c] Department of Physics, Dong Thap University, Dong Thap, Viet Nam

ARTICLE INFO

Article history:
Received 8 August 2014
Received in revised form
29 August 2014
Accepted 1 September 2014
Available online 16 September 2014

Keywords:
Nonlinear optics
Phonon-assisted cyclotron resonance
Linewidth

ABSTRACT

We theoretically study the nonlinear optical absorption phenomenon in a GaAs/GaAlAs parabolic quantum well via investigating the phonon-assisted cyclotron resonance (PACR) effect. We find that the two-photon absorption process (nonlinear) is comparable with the one-photon process (linear), and cannot be neglected in studying PACR effect. The additional peaks in the absorption spectrum due to transitions between Landau levels and electric subband energy accompanied by emission and absorption of LO-phonon are indicated. PACR behavior is strongly affected by the magnetic field, the temperature and the confinement frequency. The present work obtains an usefully resonant condition which is more general than and includes the previous resonant behaviors.

1. Introduction

The multi-photon absorption process, or a nonlinear phenomenon, has been studied in a large number of papers in recent years [1–7]. In these papers, the first- and second-orders of the nonlinear optical conductivity have been obtained using the projection-diagram method. Although these results are very clear in physical interpretation and useful in the study of optical conductivity in low-dimensional systems, their analytical calculations are quite complicated. Therefore, these results have not been applied to investigate the nonlinear phenomenon, especially, in numerical calculations. In the other works, using different methods, many researchers have succeeded in studying the linear and nonlinear optical absorptions in low-dimensional semiconductor quantum systems [8–20]. The results show that the optical absorption coefficients are strongly affected by confinement potential [11,14], structural parameters of the system [8–10,13–18], hydrostatic pressure [16,17,19], and external fields [12,20]. However, these works only investigated the optical absorption process via one-photon absorption process, the two-photon absorption process is still open for further investigation.

Phonon-assisted cyclotron resonance (PACR) has been known as one of the useful tools for investigating transport behaviour of electrons in semiconductor materials under an applied magnetic field. This effect indicates the transition of electrons between Landau levels due to the absorption of photons accompanied with the absorption or emission of phonons. Since the early theoretical predictions [21] and experimental observations [22], the cyclotron resonance and PACR have been studied both theoretically and experimentally in bulk semiconductors [23–26], in quantum wells [27–32], in quantum wires [33–35], and in quantum dots [36]. However, the study of nonlinear PACR in PQW has not been found.

It is known that in GaAs/GaAlAs systems, electron interaction with polar phonon modes is of great importance [29]. Therefore, the purpose of the present work is to investigate the effects of the magnetic field, the temperature and the confinement frequency on the linear and nonlinear optical absorption spectrum in GaAs/$Ga_{1-x}Al_xAs$ PQW in the presence of electron–LO phonon interaction. Besides, the present work also obtains an useful resonant behaviour which expresses the phonon-assisted cyclotron resonance condition, including the other types of resonances, such as the optically detected electrophonon resonance [37,38] and the optically detected magnetophonon resonance [39]. The paper is organized as follows: in Section 2, the theoretical framework used in calculations and the analytical results are presented. The discussion of the results is given in Section 3. Finally, the conclusion is given in Section 4.

2. Theoretical framework and analytical results

When an electromagnetic wave characterized by a time-dependence electric field of amplitude F_0 and angular frequency

* Corresponding author at: Department of Physics, Dong Thap University, Dong Thap, Viet Nam. Tel.: +84 67 3882919.
E-mail address: hvphuc@dthu.edu.vn (H.V. Phuc).

http://dx.doi.org/10.1016/j.optcom.2014.09.004

Ω is applied to a semiconductor system, the optical absorption power is given by [31]

$$P(\Omega)=\frac{F_0^2\sqrt{\varepsilon}}{8\pi}\sum_i W_i f_i, \tag{1}$$

where ε is the dielectric constant of the medium, f_i is the electron distribution function, and W_i is the transition probability. The sum is taken over all the initial states i of electrons. The transition probability of absorbing photon with simultaneously absorbing and/or emitting phonon $W_i^{\mp}$ can be written as [31,40]

$$W_i^{\mp}=\frac{2\pi}{\hbar}\sum_f\sum_{\mathbf{q}}|M_{fi}|^2\sum_{\ell=-\infty}^{+\infty}\frac{1}{(\ell!)^2}\left(\frac{a_0 q_\perp}{2}\right)^{2\ell}\times\delta(E_f-E_i\mp\hbar\omega_{\mathbf{q}}-\ell\hbar\Omega), \tag{2}$$

where the upper $(-)$ and lower sign $(+)$ refer to the phonon absorption and phonon emission, respectively, M_{fi} is the transition matrix element of the electron–phonon interaction, a_0 is the laser dressing parameter, $E_i\equiv E_{N,n}$ and $E_f\equiv E_{N',n'}$ are the energy initial and final states of the electron, respectively, and $\mathbf{q}=(q_z,q_\perp)$ is the phonon wave vector.

We consider a PQW, in which electron system is confined in z-direction by the potential $U(z)=m^*\omega_z^2 z^2/2$, where ω_z is the confinement frequency. When a static magnetic field $\mathbf{B}=(0,0,B)$ is applied to system, the normalized eigenfunctions in the Landau gauge for the vector potential $\mathbf{A}=(0,Bx,0)$ and the corresponding energy are given by [41]

$$|N,n,k_y\rangle=\frac{1}{\sqrt{L_y}}\exp(ik_y y)\phi_N(x-x_0)\psi_n(z), \tag{3}$$

$$E_{N,n}=\left(N+\frac{1}{2}\right)\hbar\omega_c+\varepsilon_n,\quad N=0,1,2,\ldots, \tag{4}$$

where m^* is the effective mass of a conduction electron, N and n are the Landau level index and the level quantized number in z-direction, respectively; and $\omega_c=eB/m^*$ is the cyclotron frequency. Also, $\phi_N(x-x_0)$ represents the harmonic oscillator wave function, centered at $x_0=-k_y/m^*\omega_c$. Here k_y and L_y are the wave vector and the normalization length in y-direction, respectively. The radius of the orbit in the (x,y) plane is $a_c=(\hbar/m^*\omega_c)^{1/2}$. In Eqs. (3) and (4), the one-electron normalized eigenfunctions and the corresponding eigenvalues in the conduction band are, respectively, given by

$$\psi_n(z)=\left(\frac{1}{2^n n!\sqrt{\pi}a_z}\right)^{1/2}\exp\left(-\frac{z^2}{2a_z^2}\right)H_n\left(\frac{z}{a_z}\right), \tag{5}$$

$$\varepsilon_n=\left(n+\frac{1}{2}\right)\hbar\omega_z,\quad n=0,1,2,\ldots, \tag{6}$$

where $H_n(x)$ is the nth Hermite polynomial and $a_z=(\hbar/m^*\omega_z)^{1/2}$.

The matrix elements for electron-confined LO-phonon interaction in PQW in the presence of magnetic field can be written as

$$|M_{fi}|^2=|V_m(q)|^2|J_{nn'}(q_z)|^2|J_{NN'}(q_\perp)|^2\times(N_{Li}+1/2\mp 1/2)\delta_{k_z',k_z\pm q_z}, \tag{7}$$

where N_{Li} is the distribution function of confined LO-phonon for frequency $\omega_{\mathbf{q}}=\omega_{Li}$, and the coupling function is given by [42]

$$|V_m(q)|^2=\frac{e^2\hbar\omega_{Li}}{\varepsilon_0 d_i}\left(\frac{1}{\chi_{\infty i}}-\frac{1}{\chi_{0i}}\right)\times\left(q_\perp^2+\frac{m^2\pi^2}{d_i^2}\right)^{-1},\quad m=1,2,3,\ldots, \tag{8}$$

with ε_0 is the permittivity of free space, $\chi_{\infty i}$ (χ_{0i}) and d_i are the high (low) frequency dielectric constants and the thickness of region i of quantum well, respectively, and

$$|J_{nn'}(q_{zm})|^2=\frac{n!}{n'!}e^{-a_z^2q_{zm}^2/2}(a_z^2q_{zm}^2/2)^{n'-n}\times\left[L_n^{n'-n}(a_z^2q_{zm}^2/2)\right]^2,\quad n\le n', \tag{9}$$

$$|J_{NN'}(q_\perp)|^2=\frac{N!}{N'!}e^{-a_c^2q_\perp^2/2}(a_c^2q_\perp^2/2)^{N'-N}\times\left[L_N^{N'-N}(a_c^2q_\perp^2/2)\right]^2,\quad N\le N', \tag{10}$$

where we have denoted $q_{zm}=m\pi/d_i$, and $L_N^M(x)$ is the associated Laguerre polynomials.

The transition probability in Eq. (2) contains contributions of absorption process of ℓ-photons. In this paper, we restrict ourselves to considering the process of absorbing two photons ($\ell=1,2$). Using Eq. (1) and making a straight forward calculation of probability with the use of matrix element for confined LO-phonon scattering (Eq. (7)), we obtain the expression for the optical absorption power in PQW in the case of non-degenerate electron gas

$$\begin{aligned}P(\Omega)=A(\Omega,\omega_c)\sum_{N,N',n,n'}|I_{nn'}|e^{-E_{N,n}/k_BT}\times\{[N_{Li}\delta(p\hbar\omega_c+\Delta\varepsilon_{n'n}-\hbar\omega_{Li}-\hbar\Omega)\\+(N_{Li}+1)\delta(p\hbar\omega_c+\Delta\varepsilon_{n'n}+\hbar\omega_{Li}-\hbar\Omega)]\\+(N+N'+1)\frac{a_0^2}{8a_c^2}[N_{Li}\delta(p\hbar\omega_c+\Delta\varepsilon_{n'n}\\-\hbar\omega_{Li}-2\hbar\Omega)+(N_{Li}+1)\delta(p\hbar\omega_c+\Delta\varepsilon_{n'n}+\hbar\omega_{Li}-2\hbar\Omega)]\},\end{aligned} \tag{11}$$

here we denoted $p=N'-N$ (is an integer), and $\Delta\varepsilon_{n'n}=\varepsilon_{n'}-\varepsilon_n=(n'-n)\hbar\omega_z$. In Eq. (11), the overlap integral $I_{nn'}$ is defined as

$$I_{nn'}=\sum_{m=1,2,3,\ldots}\left|J_{nn'}\left(\frac{m\pi}{d_i}\right)\right|^2, \tag{12}$$

and

$$A(\Omega,\omega_c)=\frac{F_0^2\sqrt{\varepsilon}n_eV_0^2a_0^2e^2\omega_{Li}}{128\pi^3L_zd_i\lambda a_c^6\varepsilon_0}\left(\frac{1}{\chi_{\infty i}}-\frac{1}{\chi_{0i}}\right),\quad\lambda=\sum_{N,n}e^{-E_{N,n}/k_BT}$$

with n_e is the electron concentration, k_B is the Boltzmann constant, T is the temperature. In Eq. (11), the delta functions present the energy conservation law. This implies that when an electron undergoes a collision by absorbing photon energy, its energy can only change by an amount equal to the energy of a phonon involved in the transitions. The energy-conservation delta functions in Eq. (11) show resonant behaviour at the PARC condition for PQW based on the following selection rule of transition condition:

$$\ell\hbar\Omega=p\hbar\omega_c+\Delta\varepsilon_{n'n}\pm\hbar\omega_{Li}. \tag{13}$$

This condition predicates that the PACR is affected by both Landau and electric subband levels. In the case of transitions without electric subband levels, this equation reduces to $\ell\hbar\Omega=p\hbar\omega_c\pm\hbar\omega_{Li}$. This is the pure PACR condition which is only affected by the Landau levels [31]. Furthermore, we also see that the transition condition in Eq. (13) can include the other resonant behaviours, such as the optically detected electrophonon resonance (ODEPR) [37,38], and the optically detected magnetophonon resonance (ODMPR) [39]. Indeed, being only affected by the electric subband levels, ODEPR, which satisfies the condition $\hbar\Omega=\Delta\varepsilon_{n'n}\pm\hbar\omega_{Li}$, is the specific case of PACR condition in the case of $\ell=1,p=0$. Similarly, satisfying the condition $p\hbar\omega_c=\hbar\omega_{Li}+\Delta\varepsilon_{n'n}\pm\hbar\Omega$, ODMPR is the specific case of PACR condition with $\ell=1$. Therefore, it can be seen that our PACR condition is more general than the previous ones.

Following the collision broadening model, the delta functions in Eq. (11) are replaced with Lorentzians [43]

$$\delta(Z_\ell^{\pm})=\frac{1}{\pi}\frac{\hbar\Gamma_\ell^{\mp}}{(Z_\ell^{\pm})^2+\hbar^2(\Gamma_\ell^{\mp})^2}, \tag{14}$$

where

$$Z_{\ell}^{\pm} = p\hbar\omega_c + \Delta\varepsilon_{n'n} \pm \hbar\omega_{Li} - \ell\hbar\Omega \quad (\ell = 1, 2), \tag{15}$$

and $\Gamma_{\ell}^{\mp}$ is the inverse relaxation time of electrons

$$(\Gamma_{\ell}^{\mp})^2 = \frac{|I_{nn'}|e^2\omega_{Li}}{8\pi^2 d_i \hbar p \varepsilon_0}\left(\frac{1}{\chi_{\infty i}} - \frac{1}{\chi_{0i}}\right) \times (N_{Li} + 1/2 \mp 1/2), \quad p \neq 0. \tag{16}$$

The present result yields a more specific and significant interpretation of the electronic processes for emission and absorption of phonons and photons under the applied magnetic field in GaAs/$Ga_{1-x}Al_xAs$ PQW. In the next section, we will consider the numerical evaluation in more detail.

3. Numerical results and discussion

For the numerical calculations, we take the following values as the input parameter [13,37,44]: $\varepsilon = 12.5$, $\chi_\infty = 10.89$, $\chi_0 = 13.18$, $m^* = 0.067m_e$, m_e being the mass of free electron, $\hbar\omega_0 = 36.25$ meV, $n_e = 10^{23}\ \mathrm{m}^{-3}$, and $a_0 = 5$ nm for GaAs, and $m^* = (0.067 + 0.083x)m_e$, $\hbar\omega_{Li} = (36.25 + 1.83x + 17.12x^2 - 5.11x^3)$ meV, $\chi_{0i} = 13.18 - 3.12x$, $\chi_{\infty i} = 10.89 - 2.73x$ for $Ga_{1-x}Al_xAs$ [42].

In Fig. 1 we show the dependence of the absorption power on photon energy at B=9 T, which leads to the cyclotron energy $\hbar\omega_c = 15.65$ meV in the well GaAs and 10.46 meV in the barrier $Ga_{0.6}Al_{0.4}As$, respectively. These peaks are due to PACR, which represents resonance transfer of electrons with absorption of photons accompanied with the absorption/emission of phonons. Depending upon the Landau level and electric subband separations, photon, and phonon energies, the PACR transitions have various types [29]. For a magnetic field B=9 T, the cyclotron energy is smaller than the LO-phonon energy, the transitions correspond to the type 2 in Ref. [29].

Using the computational method, we easily determine that the peaks at $\hbar\Omega = 66.40$ meV, 82.05 meV and 97.70 meV of the solid line satisfy the condition $\Omega = p\omega_c + \omega_z + \omega_0$, with p=1, 2 and 3, respectively. These three peaks correspond to the one-photon process (linear phenomenon). Moreover, the peak value of absorption power at p=2 and 3 is about 52% and 34%, respectively, of that at p=1. At $\hbar\Omega = 33.20$ meV, 41.03 meV, and 48.85 meV, the peaks satisfy the condition $2\Omega = p\omega_c + \omega_z + \omega_0$, with p=1, 2 and 3, respectively, describing the two-photon process (nonlinear phenomenon). In the nonlinear case, the peak values at p=2 and p=3 are about 79% and 73.7%, of that at p=1, respectively. Besides, the peak values in the nonlinear process are about 26%, 40%, and 56%, respectively, of that in the linear process at p=1,2, and p=3.

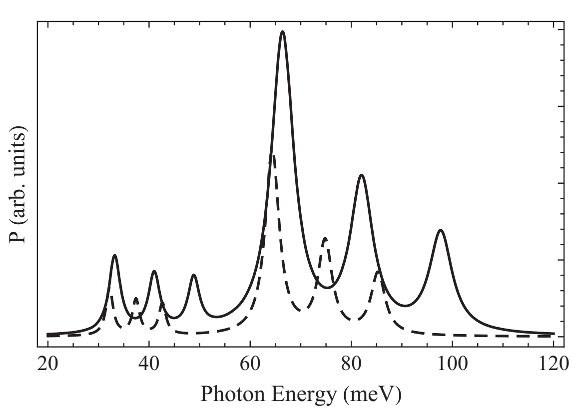

Fig. 1. Absorption power as a function of the photon energy in a PQW with a confinement frequency $\omega_z/\omega_0 = 0.4$ at B=9 T, d_i=50 Å, and T=77 K. The solid and dashed lines present the absorption power in the well GaAs, and the barrier $Ga_{0.6}Al_{0.4}As$ (x=0.4), respectively.

Therefore, the nonlinear absorption process is strong enough to be detected in PACR.

In the barrier $Ga_{0.6}Al_{0.4}As$, the phenomenon occurs similarly, but the resonance peaks seem to give a red-shift. This resulted in the effective mass of electron and confined LO-phonon energy which are modified in $Ga_{0.6}Al_{0.4}As$. In detail, for x=0.4, the effective mass $m^* = 0.1m_e$ leading to cyclotron energy $\hbar\omega_c = 10.46$ meV, and $\hbar\omega_{Li} = 39.39$ meV. Therefore, the resonant peak occurring at $\hbar\Omega = 64.4$ meV satisfies the condition $\Omega = p\omega_c + \omega_z + \omega_{Li}$, with p=1. This value of the resonant peak is smaller than that in GaAs (66.40 meV). This explains the red-shift behavior of the absorption spectrum in the barrier $Ga_{0.6}Al_{0.4}As$. The others peaks of the dashed line can be explained similarly.

In Fig. 2, we depict the absorption power in the well GaAs as functions of photon energy for different values of magnetic field. It is possible to see that the increase in the value of magnetic field leads to a blue-shift of the resonant peaks. The physical meaning of this phenomenon is that when the magnetic field increases, the Landau level separation becomes larger resulting in the increase of the value of absorbed photon energy.

Fig. 3 shows the dependence of PACR absorption spectrum on the temperature. We can see from the figure that the PACR peaks are located at the same position but the peak values of absorption power are seen to increase with the temperature. As the temperature increases, the electron–phonon scattering increases, leading to a general increase in the temperature of absorption power.

Fig. 4 shows the dependence of PACR absorption spectrum on the confinement frequency. In the figure, when the confinement frequency increases, the PACR peaks are seen to shift to the large region of the photon energy (blue-shift). As the confinement frequency increases, the electric subband separation energy increases, leading to the increasing of the value of absorbed photon energy.

For the PACR-linewidth, using profile method [45] we obtain the magnetic field dependence of the PACR-linewidth, as shown in Fig. 5. It can be found that both the well and barrier PACR-linewidth increase with increasing magnetic field B. The reason for this is that the electron–phonon interaction increases when magnetic field increases. This result is in good agreement with the results of previous papers [25–27,32,34]. The physical meaning of this phenomenon can be explained as follows: when magnetic field B increases, the cyclotron radius a_c reduces, the confinement of electron increases, the probability of electron–phonon scattering increases, leading to the increasing of the linewidth. In addition, we can also see from the figure that PACR-linewidth varies with the square root of magnetic field, agreeing with the previous result [27]. Besides, the linewidth in nonlinear absorption process is about 51% of that in linear one for the well and 49% for

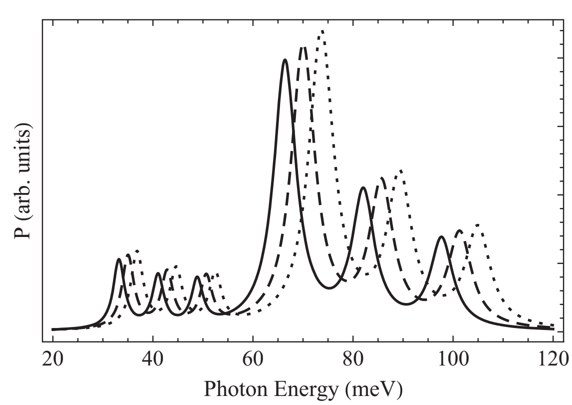

Fig. 2. Absorption power is shown as a function of photon energy for different values of magnetic field. The solid, dashed, and dotted curves correspond to B=9 T, 10 T, and 11 T. Here T=77 K, d_i=50 Å, and $\omega_z/\omega_0 = 0.4$.

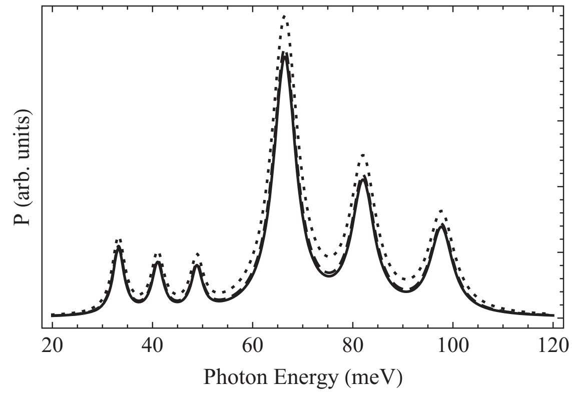

Fig. 3. Absorption power is shown as a function of photon energy for different values of temperature. The solid, dashed, and dotted curves correspond to $T=77$ K, 150 K, and 300 K. Here $B=9$ T, $d_i=50$ Å, and $\omega_z/\omega_0=0.4$.

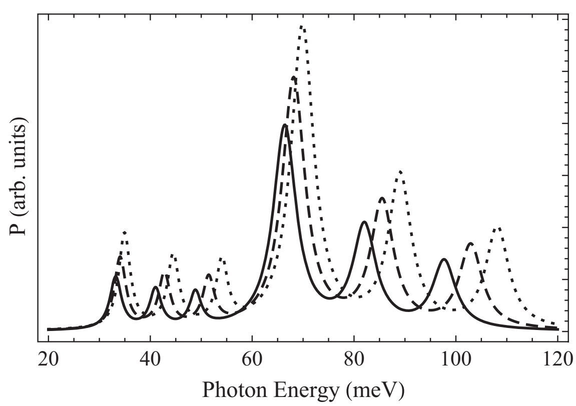

Fig. 4. Absorption power is shown as a function of photon energy for different values of confinement frequency. The solid, dashed, and dotted curves correspond to $\omega_z/\omega_0=0.4$, 0.5, and 0.6. Here $B=9$ T, $d_i=50$ Å, and $T=77$ K.

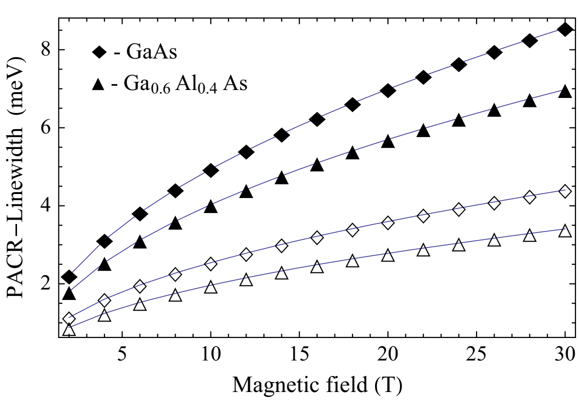

Fig. 5. Dependence of the PACR-linewidth on the magnetic field at $T=77$ K, $d_i=50$ Å, and $\omega_z/\omega_0=0.4$. The diamond and triangle lines present the linewidth in the well GaAs and the barrier $Ga_{0.6}Al_{0.4}As$, the filled and empty lines correspond to the linear and nonlinear absorption process, respectively.

the barrier. Therefore, this result once again shows that the nonlinear absorption process is strong enough to be detected, and cannot be neglected in studying the PACR-linewidth in PQW.

Fig. 6 shows the temperature dependence of the PACR-linewidth. It is seen from the figure that the PACR-linewidth varies with the square root of temperature. This result is in good agreement with the result of the paper of Chaubey and Van Vliet [27]. As the temperature increases, probability of electron–phonon scattering increases, leading to a general increase in the temperature of PACR-linewidth. The

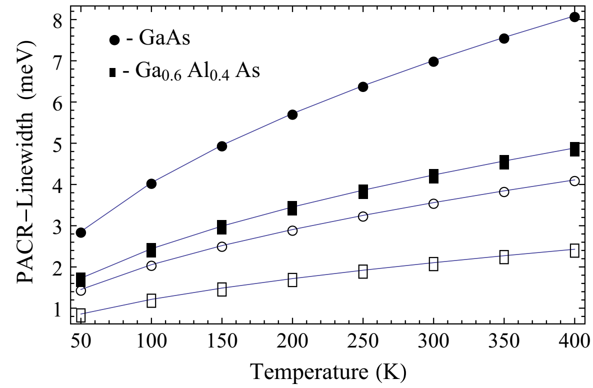

Fig. 6. Dependence of the PACR-linewidth on the temperature at $B=9$ T, $d_i=50$ Å, and $\omega_z/\omega_0=0.4$. The circle and rectangular lines present the linewidth in the well GaAs and the barrier $Ga_{0.6}Al_{0.4}As$, the filled and empty lines correspond to the linear and nonlinear absorption process, respectively.

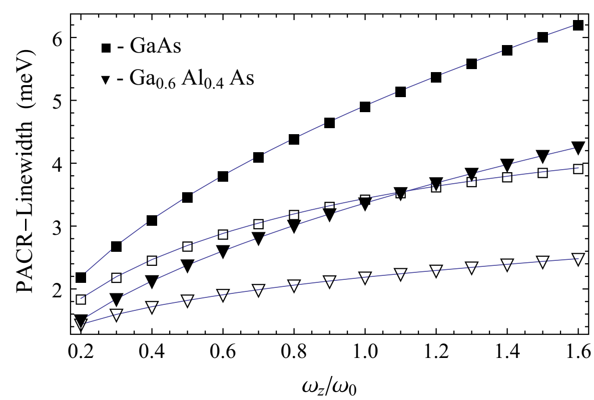

Fig. 7. Dependence of the PACR-linewidth on the confinement frequency at $B=9$ T, $d_i=50$ Å, and $T=77$ K. The square and down-triangle lines present the linewidth in the well GaAs and the barrier $Ga_{0.6}Al_{0.4}As$, the filled and empty lines correspond to the linear and nonlinear absorption process, respectively.

linewidth in nonlinear absorption process is about 50% of that in linear one in both the well GaAs and the barrier $Ga_{0.6}Al_{0.4}As$.

Fig. 7 shows the dependence of PACR-linewidth on the confinement frequency at $B=9$ T, and $T=77$ K. From the figure, we can see that the PACR-linewidth increases with the confinement frequency for both linear and nonlinear absorption process. Furthermore, the PACR-linewith in the linear process varies faster and has a larger value than it does in comparison with the nonlinear process. In this case, the linewidth in the nonlinear absorption process is from about 84% (95%) at $\omega_z/\omega_0=0.2$ to 63% (58%) at $\omega_z/\omega_0=1.6$ of that in the linear one for the well GaAs (the barrier $Ga_{0.6}Al_{0.4}As$). Finally, we can see that the PACR-linewidth in the barrier is always smaller than that in the well in each case associated.

4. Conclusion

In the present work, we have studied the PACR in GaAs/GaAlAs PQW by considering the two-photon absorption process when electrons interact with LO-phonons. The absorption spectrum satisfies the condition $\ell\hbar\Omega=p\hbar\omega_c+\Delta\varepsilon_{n'n}\pm\hbar\omega_{Li}$, and can include the other resonant behaviours. The results show that the PACR behaviour is affected by the magnetic field, the temperature and confinement frequency.

Using profile method, we obtained the PACR-linewidth as profile of the curves. The values of the PACR-linewidth are found to increase with the increase of magnetic field, temperature and confinement frequency. Although being smaller than the linear absorption process, the nonlinear process is strong enough to be detected in PACR, and cannot be neglected in studying the PACR-linewidth. Unfortunately, up to now, there are no relevant experimental result for comparing to our theory. We hope that new experiments will test the validity of our prediction in a very near future.

Acknowledgments

The authors would like to thank the anonymous reviewers for their helpful and constructive comments that greatly contributed to improving the paper.

Appendix A. Supplementary data

Supplementary data associated with this paper can be found in the online version at http://dx.doi.org/10.1016/j.optcom.2014.09.004.

References

[1] H.J. Lee, N.L. Kang, J.Y. Sug, S.D. Choi, Phys. Rev. B 65 (2002) 195113.
[2] N.L. Kang, S.D. Choi, J. Phys. A: Math. Theor. 43 (2010) 165203.
[3] N.L. Kang, Y.J. Lee, S.D. Choi, J. Korean Phys. Soc. 58 (2011) 538.
[4] N.L. Kang, S.D. Choi, J. Mod. Phys. 2 (2011) 1410.
[5] N.L. Kang, S.D. Choi, Prog. Theor. Phys. 125 (2011) 1011.
[6] N.L. Kang, S.D. Choi, AIP Adv. 2 (2012) 012161.
[7] N.L. Kang, S.-S. Lee, S.D. Choi, AIP Adv. 3 (2013) 072104.
[8] A. Keshavarz, M. Karimi, Phys. Lett. A 374 (2010) 2675.
[9] L.T.T. Phuong, H.V. Phuc, T.C. Phong, Comput. Mater. Sci. 49 (2010) S260.
[10] R. Khordad, S. Tafaroji, Physica E 46 (2012) 84.
[11] W. Xie, Opt. Commun. 284 (2011) 5730.
[12] F. Ungan, U. Yesilgul, E. Kasapoglu, H. Sari, I. Sokmen, J. Lumin. 132 (2012) 1627.
[13] U. Yesilgul, J. Lumin. 132 (3) (2012) 765.
[14] Y. Yakar, B. akr, A. zmen, Opt. Commun. 283 (2010) 1795.
[15] E. Ozturk, Y. Ozdemir, Opt. Commun. 294 (2013) 361.
[16] R. Restrepo, M. Barseghyan, M. Mora-Ramos, C. Duque, Physica E 51 (2013) 48.
[17] H. Baghramyan, M. Barseghyan, A. Kirakosyan, R. Restrepo, C. Duque, J. Lumin. 134 (2013) 594.
[18] H. Baghramyan, M. Barseghyan, A. Kirakosyan, R. Restrepo, M. Mora-Ramos, C. Duque, J. Lumin. 145 (2014) 676.
[19] V. Mughnetsyan, A. Manaselyan, M. Barseghyan, A. Kirakosyan, J. Lumin. 134 (2013) 24.
[20] E.C. Niculescu, N. Eseanu, A. Radu, Opt. Commun. 294 (2013) 276.
[21] F.G. Bass, I.B. Levinson, Sov. Phys. JETP 22 (1966) 635.
[22] R.C. Enck, A.S. Saleh, H.Y. Fan, Phys. Rev. 182 (1969) 790.
[23] Y.J. Cho, S.D. Choi, Phys. Rev. B 49 (1994) 14301.
[24] T.M. Rynne, H.N. Spector, J. Appl. Phys. 52 (1981) 393.
[25] J.Y. Sug, S.G. Jo, J. Kim, J.H. Lee, S.D. Choi, Phys. Rev. B 64 (2001) 235210.
[26] H. Kobori, T. Ohyama, E. Otsuka, J. Phys. Soc. Jpn. 59 (1990) 2141.
[27] M.P. Chaubey, C.M. Van Vliet, Phys. Rev. B 34 (1986) 3932.
[28] J.S. Bhat, S.S. Kubakaddi, B.G. Mulimani, J. Appl. Phys. 70 (1991) 2216.
[29] J.S. Bhat, B.G. Mulimani, S.S. Kubakaddi, Phys. Rev. B 49 (1994) 16459.
[30] Y.B. Vasilyev, S.D. Suchalkin, S.V. Ivanov, B.Y. Meltser, P.S. Kop'ev, Phys. Status Solidi B 240 (2003) R8.
[31] H.V. Phuc, L. Dinh, T.C. Phong, Superlattices Microstruct. 59 (2013) 77.
[32] H.V. Phuc, L.V. Tung, Superlattices Microstruct. 71 (2014) 124.
[33] V.A. Margulis, A.V. Shorokhov, Phys. Status Solidi C 1 (2004) 2642.
[34] H.V. Phuc, L.T.M. Hue, L. Dinh, T.C. Phong, Superlattices Microstruct. 60 (2013) 508.
[35] R. Betancourt-Riera, R. Betancourt-Riera, J.N. Jalil, R. Riera, Physica B 410 (2013) 126.
[36] S.-H. Chen, Physica E 43 (2011) 1007.
[37] S.C. Lee, J.W. Kang, H.S. Ahn, M. Yang, N.L. Kang, S.W. Kim, Physica E 28 (2005) 402.
[38] L.T.T. Phuong, H.V. Phuc, T.C. Phong, Physica E 56 (2014) 102.
[39] S.C. Lee, J. Korean Phys. Soc. 51 (2007) 1979.
[40] W. Xu, R.A. Lewis, P.M. Koenraad, C.J.G.M. Langerak, J. Phys.: Condens. Matter 16 (2004) 89.
[41] R. Haupt, L. Wendler, Solid State Commun. 89 (1994) 741.
[42] J. Gong, X.X. Liang, S.L. Ban, J. Appl. Phys. 100 (2006) 023707.
[43] M.P. Chaubey, C.M. Van Vliet, Phys. Rev. B 33 (1986) 5617.
[44] X. Yu, Y. Yu, Superlattices Microstruct. 62 (2013) 225.
[45] T.C. Phong, H.V. Phuc, Mod. Phys. Lett. B 25 (2011) 1003.